Takashi Nomiyama,[1] Takako Kawanami,[1] Shinichiro Irie,[2] Yuriko Hamaguchi,[1] Yuichi Terawaki,[1] Kunitaka Murase,[1] Yoko Tsutsumi,[1] Ryoko Nagaishi,[1] Makito Tanabe,[1] Hidetaka Morinaga,[1] Tomoko Tanaka,[1] Makio Mizoguchi,[3] Kazuki Nabeshima,[3] Masatoshi Tanaka,[2] and Toshihiko Yanase[1]

Exendin-4, a GLP-1 Receptor Agonist, Attenuates Prostate Cancer Growth

Diabetes 2014;63:3891–3905 | DOI: 10.2337/db13-1169

Recently, pleiotropic benefits of incretin therapy beyond glycemic control have been reported. Although cancer is one of the main causes of death in diabetic patients, few reports describe the anticancer effects of incretin. Here, we examined the effect of the incretin drug exendin (Ex)-4, a GLP-1 receptor (GLP-1R) agonist, on prostate cancer. In human prostate cancer tissue obtained from patients after they had undergone radical prostatectomy, GLP-1R expression colocalized with P504S, a marker of prostate cancer. In in vitro experiments, Ex-4 significantly decreased the proliferation of the prostate cancer cell lines LNCap, PC3, and DU145, but not that of ALVA-41. This antiproliferative effect depended on GLP-1R expression. In accordance with the abundant expression of GLP-1R in LNCap cells, a GLP-1R antagonist or *GLP-1R* knockdown with small interfering RNA abolished the inhibitory effect of Ex-4 on cell proliferation. Although Ex-4 had no effect on either androgen receptor activation or apoptosis, it decreased extracellular signal–regulated kinase (ERK)-mitogen-activated protein kinase (MAPK) phosphorylation in LNCap cells. Importantly, Ex-4 attenuated in vivo prostate cancer growth induced by transplantation of LNCap cells into athymic mice and significantly reduced the tumor expression of P504S, Ki67, and phosphorylated ERK-MAPK. These data suggest that Ex-4 attenuates prostate cancer growth through the inhibition of ERK-MAPK activation.

Incretin therapy, which includes the delivery of dipeptidyl peptidase-4 inhibitors and GLP-1 receptor (GLP-1R) agonists, has become a popular treatment for type 2 diabetes. Recently, much attention has focused on incretin because of its reported tissue-protective effects beyond lowering glucose levels (1). Diabetic patients have a higher risk of cardiovascular events compared with nondiabetic patients (2) and frequently experience restenosis after coronary angioplasty, even if intervention is performed with currently established drug-eluting stents (3). Accordingly, the potential of incretin-related antidiabetic agents to improve not only glycemic control but also cardiovascular systems has been investigated. Indeed, the vascular protective effects of exendin (Ex)-4, a GLP-1R agonist, have been demonstrated by the attenuation of atheroma formation in apoE$^{-/-}$ mice via inhibition of nuclear factor-κB activation in macrophages (4) and by the reduction in intimal thickening after vascular injury via 5′ AMPK activation in vascular smooth muscle cells (5). Thus, incretin therapy could improve the quality of life and mortality rate of patients with diabetes through its vascular protective effects.

Cancer is another major cause of death in diabetic patients (6), especially in Japan, where it is the leading cause of death in patients with type 2 diabetes (7). Subsequently, the Japan Diabetes Society and Japanese Cancer Association have issued a warning about increased risk of cancer in diabetic patients (8). Furthermore, the Hisayama study has suggested (9) that not only diabetes but also impaired glucose tolerance increases the incidence of cancer-related deaths in the Japanese population. Specifically, diabetes has been suggested to be associated with

[1]Department of Endocrinology and Diabetes Mellitus, School of Medicine, Fukuoka University, Jonan-ku, Fukuoka, Japan
[2]Department of Urology, School of Medicine, Fukuoka University, Jonan-ku, Fukuoka, Japan
[3]Department of Pathology, Faculty of Medicine, Fukuoka University, Jonan-ku, Fukuoka, Japan
Corresponding author: Toshihiko Yanase, tyanase@fukuoka-u.ac.jp.

Received 29 July 2013 and accepted 27 May 2014.
This article contains Supplementary Data online at http://diabetes.diabetesjournals.org/lookup/suppl/doi:10.2337/db13-1169/-/DC1.
T.N. and T.K. contributed equally to this work.

a higher risk for many malignancies, such as pancreatic (10), renal cell (11), colon (12), and breast (13) cancers.

Although numerous types of cancer have been recognized to be associated with diabetes and metabolic syndrome (14), the association of diabetes and metabolic syndrome with prostate cancer remains controversial (15–19). Indeed, diabetes has been associated with both advanced prostate cancer and prostate cancer mortality, but not with the total phenomena caused by prostate cancer. Moreover, a follow-up study of 2,546 patients with prostate cancer who were enrolled in the Physicians' Health Study (20) revealed that both high BMI values and high plasma C-peptide concentrations increased the risk of mortality (21). Furthermore, we have previously reported that insulin and IGF-I accelerate prostate cancer cell proliferation through androgen receptor (AR) activation by disrupting its direct interaction with FOXO1 (22). These data favor the hypothesis that insulin resistance and hyperinsulinemia in prediabetic or early diabetic states and metabolic syndrome are associated with poor prognosis for prostate cancer patients. Intensive treatment of diabetes is, therefore, a rationale for preventing cancer (23). In the current study, we examined the anticancer effect of antidiabetic incretin treatment using Ex-4 in a prostate cancer model. We found that Ex-4 attenuated prostate cancer growth through the inhibition of extracellular signal–regulated kinase (ERK)-mitogen-activated protein kinase (MAPK) activation.

RESEARCH DESIGN AND METHODS

Human Tissue

Human prostate cancer tissue samples were obtained from two nondiabetic prostate cancer patients (67 and 70 years old) after radical prostatectomy at the Fukuoka University Hospital. The tissue samples were paraffin embedded, formalin fixed, and cut into 3-μm sections for immunofluorescent staining. All patients provided written informed consent for participation in this study. The study protocol was approved by the Ethics Committees of Fukuoka University Hospital.

Animals

Athymic CAnN.Cg-*Foxn1nu*/CrlCrlj mice were purchased from Charles River Laboratories (Yokohama, Japan) and were housed in specific pathogen-free barrier facilities at Fukuoka University. Mice were treated with either saline solution (n = 7) or Ex-4 (Sigma-Aldrich, St. Louis, MO) at a high dose (24 nmol/kg body weight/day; n = 7) or a low dose (300 pmol/kg body weight/day; n = 8) delivered through a micro-osmotic pump (ALZET, model 1004; DURECT, Cupertino, CA), as described previously (4). At the age of 6 weeks, 1×10^6 LNCap cells (passages 4–8) were mixed with 250 μL of Matrigel (Becton Dickinson Labware, Bedford, MA), and after local anesthesia they were transplanted subcutaneously into the flank region of each mouse while the osmotic pump was inserted under the dorsal skin. At the age of 12 weeks, blood samples were collected and the mice were killed. Tumors were extracted, and their volume was calculated according to the following modified ellipsoid formula: length × width squared × 0.52, as previously reported (24). Paraffin-embedded formalin-fixed tumors were cut into 5-μm sections and prepared for immunofluorescent staining. All animal procedures were reviewed and approved by the Institutional Animal Care Subcommittee of Fukuoka University Hospital.

Cell Culture and Cell Proliferation Assays

The LNCap human androgen-sensitive prostate cancer cell line, and the PC3 and DU145 human androgen-independent prostate cancer cell lines were purchased from the American Type Culture Collection (Manassas, VA). The ALVA-41 human androgen-sensitive prostate cancer cell line was provided by Dr. Seiji Naito (Kyushu University, Fukuoka, Japan). LNCap, ALVA-41, and DU145 cells were maintained in RPMI 1640 media, and PC3 cells were cultured in DMEM Nutrient Mixture F-12. All media were supplemented with 10% FBS and 1% penicillin/streptomycin. Cell proliferation assays were performed as described previously (25) with minor modifications. Briefly, LNCap (30,000 cells/well), PC3 (60,000 cells/well), ALVA-41 (30,000 cells/well), and DU145 (30,000 cells/well) cells were seeded in 12-well tissue culture plates and maintained in complete media with or without 0.1–10 nmol/L Ex-4, 100 nmol/L Ex (9–39) (Bachem, Torrance, CA), 10 μmol/L $PKI_{14–22}$ (Sigma-Aldrich), or 10 μmol/L PD98059 (Sigma-Aldrich). Cell proliferation was analyzed daily up to 4 days by cell counting using a hemocytometer. For all experiments, cells were used at passages 4–8. Experiments were performed in triplicate using five different cell preparations.

Small Interfering RNA Knockdown of *GLP-1R* Expression and Cell Proliferation Assay

To knockdown *GLP-1R*, we used Stealth RNAi Pre-Designed small interfering RNA (siRNA) (Invitrogen, Carlsbad, CA), which was designed for human *GLP-1R* (HSS104179–81), and Stealth RNAi Negative Control Duplexes (Invitrogen) were used as a negative control. For transfection, LNCap cells were plated at a density of 1×10^5 cells/well in 6-well plates and transfected with 1 nmol/L *GLP-1R* siRNA or the negative control using MISSION siRNA Transfection Reagent (Sigma-Aldrich). Twenty-four hours after transfection, cells were subjected to the cell proliferation assay. Briefly, cells were detached and replated in 24-well tissue culture plates in complete media with or without 10 nmol/L Ex-4. Four days after the treatment, cells were collected and counted using a hemocytometer. The siRNA knockdown efficiency was confirmed by RT-PCR analysis of *GLP-1R* (Supplementary Fig. 2).

Reverse Transcription and Quantitative Real-Time RT-PCR

Total mRNA from prostate cancer cells was isolated using RNeasy Mini Kits (Qiagen, Venlo, the Netherlands) and reverse transcribed into cDNA. PCRs were performed using LightCycler 2.0 (Roche, Basel, Switzerland) and SYBR Premix Ex Taq II (Takara, Otsu, Japan). Each sample was analyzed in triplicate and normalized against TATA binding

protein (*TBP*) mRNA expression. The primer sequences used were as follows: human *TBP*, 5′-TGCTGCGGTAATC ATGAGGATA-3′ (forward), 5′-TGAAGTCCAAGAACTTAGC TGGAA-3′ (reverse); human *GLP-1R*, 5′-GGTTCATCTAGG GACACGTTAGGA-3′ (forward), 5′-GACAGCGTGTGGTCA CAGATAAAG-3′ (reverse); and human prostate serum antigen (*PSA*), 5′-CACCTGCTCGGGTGA-3′ (forward), 5′-CCACTTCCGGTAATGCACCA-3′ (reverse). To verify the mRNA expression of human *GLP-1R*, we also amplified the 890-base pair (BP) coding sequence of human *GLP-1R* using RT-PCR, as previously reported (26). PCR products were separated by agarose gel electrophoresis and visualized with ethidium bromide staining.

Determination of cAMP Concentration

Measurement of cAMP concentration was performed as described previously (5). Briefly, LNCap cells were plated in 96-well plates at a density of 1,500 cells/well and cultured overnight. Next, they were serum deprived for 24 h and incubated with Ex-4 (10 nmol/L) for 0, 15, 30, or 60 min. After incubation, the medium was aspirated and lysis buffer was added. Intracellular cAMP concentration ($[cAMP]_i$) was determined using the cAMP enzyme immunoassay (EIA) kit (GE Healthcare, Little Chalfont, U.K.) according to the manufacturer's instructions.

PSA Measurements

PSA protein concentrations in cell culture medium and mouse serum were measured using EIA at SRL Inc. (Tokyo, Japan).

Plasmids, Transient Transfections, and Luciferase Assays

To evaluate AR activation, the luciferase reporter assay was performed in LNCap cells transiently transfected with the pGL3-MMTV or phospho–PSA-LUC reporter constructs, as described previously (22). Briefly, LNCap cells were transfected for 6–8 h with 0.5 μg of reporter DNA using FuGENE HD Transfection Reagent (Roche). Next, cells were maintained in media supplemented with 10% dextran-coated charcoal-filtered FBS with or without Ex-4 (0.1–10 nmol/L) for 12 h, followed by stimulation with 10^{-8} mol/L 5α-dihydrotestosterone (DHT; Sigma-Aldrich) for 24 h. Luciferase activity was assayed using the dual luciferase reporter assay (Promega, Madison, WI). Transfection efficiency was normalized to *Renilla* luciferase activity generated by cotransfection of cells with 10 ng/well pRL-SV40 (Promega).

BrdU Assays

To evaluate LNCap cell proliferation, the BrdU incorporation assay was performed using Cell Proliferation ELISA

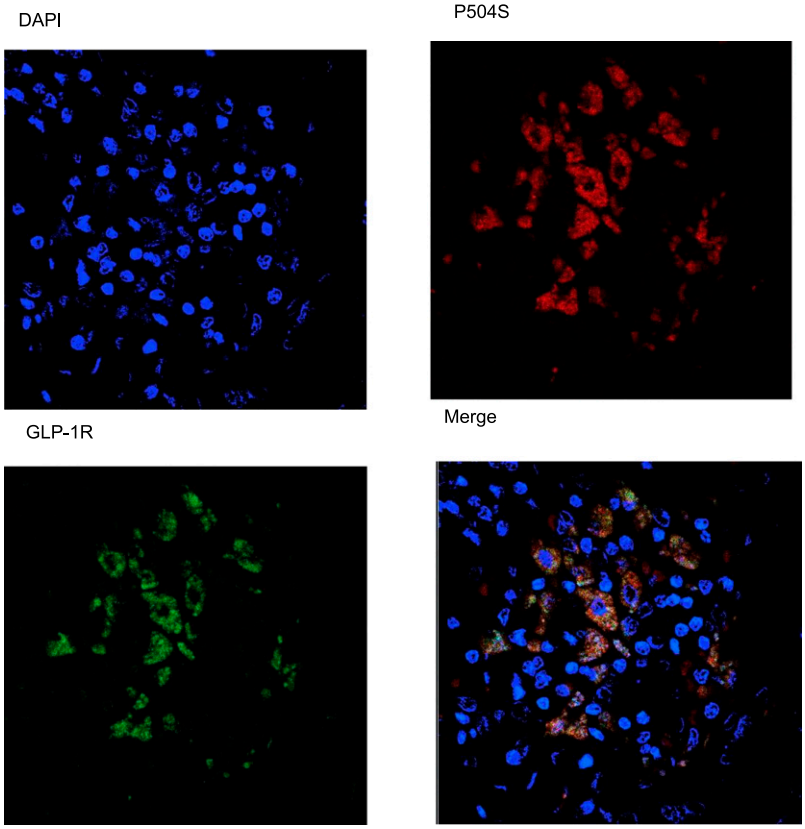

Figure 1—Expression of the GLP-1R in human prostate cancer tissue. Paraffin-embedded serial sections of human prostate cancer tissue obtained from nondiabetic prostate cancer patients were stained for the GLP-1R and P504S and counterstained with DAPI. Original magnification ×630.

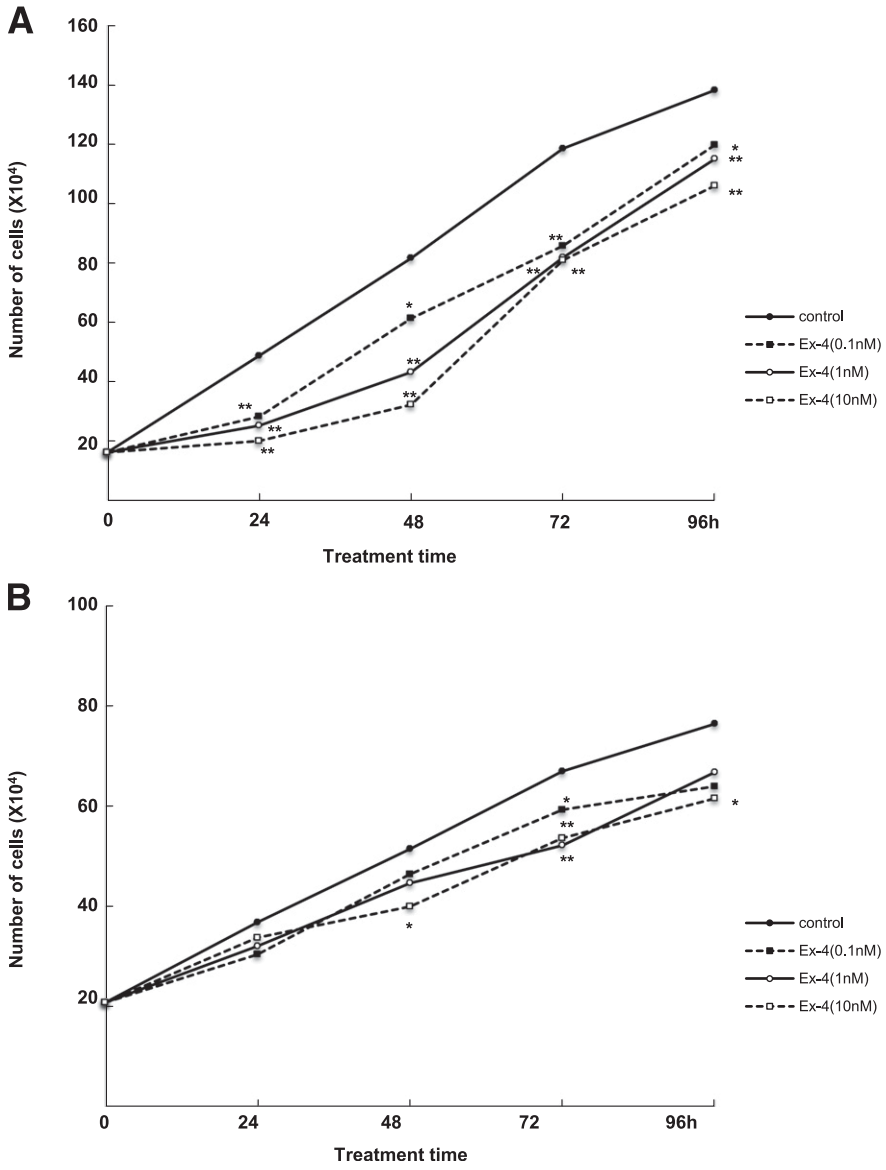

Figure 2— Ex-4 inhibits prostate cancer cell proliferation via the GLP-1R. LNCap cells (*A*), PC3 cells (*B*), ALVA-41 cells (*C*), and DU145 cells (*D*) were maintained in the recommended media supplemented with 10% FBS with or without Ex-4 (0.1–10 nmol/L). After 0, 24, 48, 72, and 96 h, the cells were harvested, and cell proliferation was analyzed by cell counting using a hemocytometer. Control (nontreated), black circles with solid line; Ex-4 (0.1 nmol/L), black squares with dotted line; Ex-4 (1 nmol/L), white circles with solid line; Ex-4 (10 nmol/L), white squares with dotted line. One-way ANOVA was performed to calculate statistical significance: $^{*}P < 0.05$ vs. control; $^{**}P < 0.01$ vs. control.

kits (1647229; Roche Applied Science, Mannheim, Germany), as described previously (5). Briefly, LNCap cells were plated at 3,000 cells/well in 96-well culture plates in complete media. After attaining 60–70% confluence, LNCap cells were treated with or without Ex-4 (0.1–10 nmol/L) diluted in media with 10% FBS for 24 h. BrdU solution (10 μmol/L) was added during the last 2 h of stimulation. Next, the cells were dried and fixed, and the cellular DNA was denatured with FixDenat solution (Roche Applied Science) for 30 min at room temperature. A peroxidase-conjugated mouse anti-BrdU monoclonal antibody (Roche Applied Science) was added to the culture plates and incubated for 90 min at room temperature. Finally, tetramethylbenzidine substrate was added for 15 min at room temperature, and the absorbance of the samples was measured using a microplate reader at 450–620 nm. Mean data are expressed as a ratio of the control (nontreated) cell proliferation.

Apoptosis Assays

For labeling nuclei of apoptotic cells, 1.2×10^5 LNCap cells were plated on glass coverslips in Lab-Tek Chamber Slides (Nunc, #177380; Thermo Scientific, Waltham, MA) and fixed in 4% paraformaldehyde for 25 min. TUNEL staining was performed using the DeadEnd Fluorometric TUNEL System (Promega) according to the

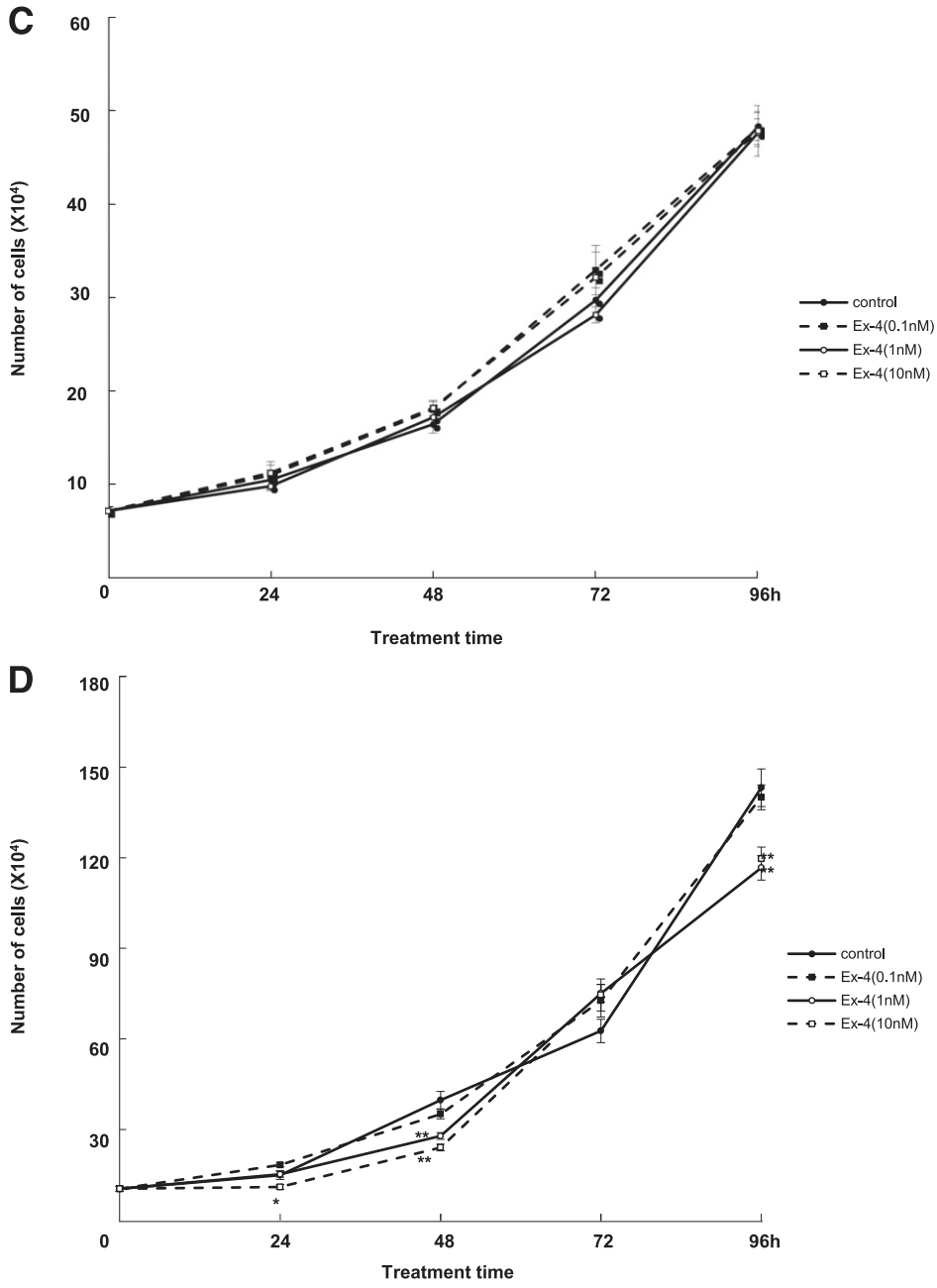

Figure 2—*Continued*.

manufacturer's protocol. During the final 24 h, LNCap cells were incubated with 10 nmol/L Ex-4. LNCap cells treated with 1 unit/100 μL RQ1 RNase-Free DNase (M6101; Promega) for 24 h were used as a positive control. Triplicate independent experiments were conducted.

Immunohistochemistry

Paraffin sections were incubated with anti–GLP-1R antibody (NBP1–97308; Novus Biologicals, Littleton, CO), anti-P504S antibody (IR060; Agilent Technologies, Santa Clara, CA), anti-Ki67 antibody (ab66144; Abcam, Cambridge, U.K.), or anti-phosphorylated (phospho) ERK-MAPK antibody (Thr-202/Tyr-204) (#4370; Cell Signaling Technology, Danvers, MA). Sections analyzed for GLP-1R and phospho–ERK-MAPK (Thr-202/Tyr-204) were subsequently incubated with Alexa Fluor 488 goat anti-rabbit IgG (A-11008; Life Technologies, Carlsbad, CA), and sections analyzed for P504S and Ki67 were subsequently incubated with Alexa Fluor 546 goat anti-rabbit IgG (A-11010; Life Technologies). Sections were counterstained with DAPI and visualized by confocal microscopy.

Western Blot Analysis

Western blotting was performed as described previously (25). The following primary antibodies were used: phospho–ERK-MAPK (Thr-202/Tyr-204) (catalog #9101;

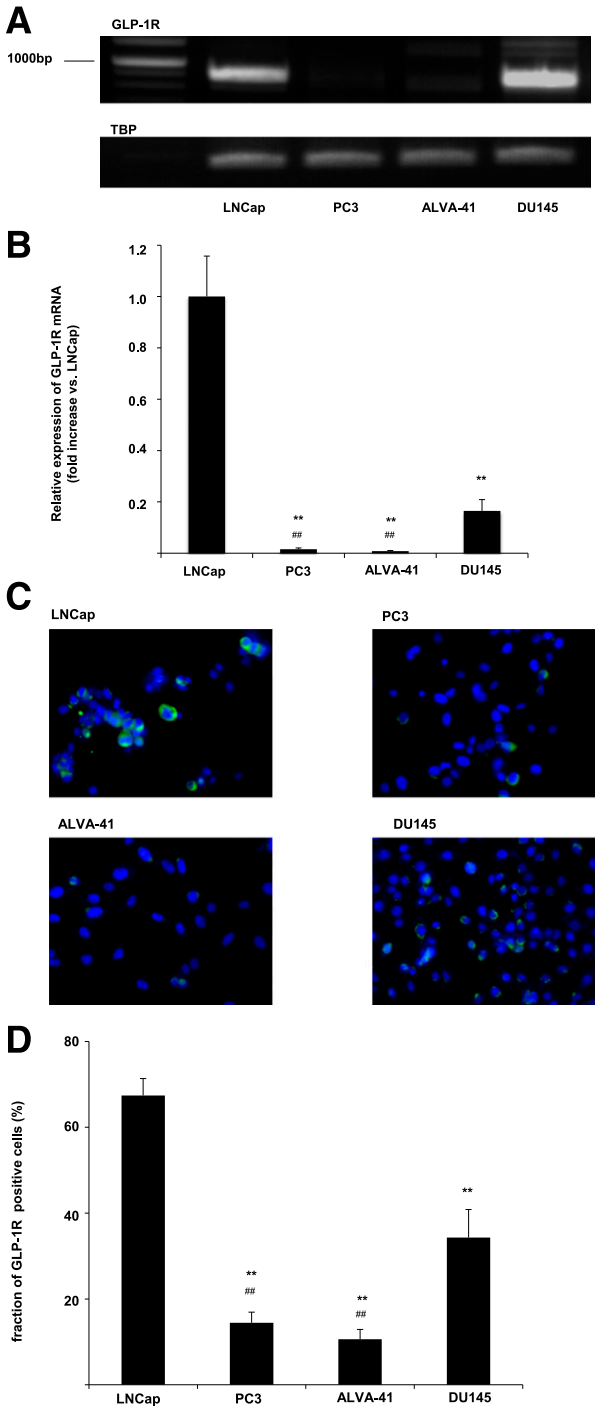

Figure 3—GLP-1R expression in prostate cancer cells. *A*: RT-PCR was performed to examine mRNA levels of an 890-BP *GLP-1R* open reading frame. *TBP* was used as an input control. *B*: Quantitative RT-PCR was performed using a set of primers targeting exon 13 of *GLP-1R*. *TBP* expression was used for normalization. Unpaired *t* tests were performed to calculate statistical significance: $^{**}P < 0.01$ vs. LNCap cells; $\#\#P < 0.01$ vs. DU145 cells. *C*: Immunohistochemistry was performed to examine GLP-1R expression in prostate cancer cell lines. All samples were counterstained with DAPI. Original magnification ×400. *D*: GLP-1R–positive cells were counted and normalized against DAPI in four individual fields of view. Unpaired *t* tests were performed to calculate statistical significance: $^{**}P < 0.01$ vs. LNCap cells; $\#\#P < 0.01$ vs. DU145 cells.

Cell Signaling Technology) and ERK-MAPK (catalog #9102; Cell Signaling Technology). The expression of these proteins was examined in LNCap cells that were incubated in media with 10% FBS and stimulated with or without 10 nmol/L Ex-4 for 15 min and pretreated for 30 min with or without 10 μmol/L cAMP protein kinase A (PKA) inhibitor (PKI) PKI_{14-22} (Sigma-Aldrich).

Statistical Analysis

Unpaired *t* tests and one-way ANOVAs were performed for statistical analysis as appropriate. *P* values <0.05 were considered to be statistically significant. Results are expressed as the mean ± SEM.

RESULTS

GLP-1R Is Expressed in Human Prostate Cancer Tissue

To assess GLP-1R expression in prostate cancer, we first performed immunohistochemical analysis of GLP-1R in human prostate cancer tissue. As shown in Fig. 1, GLP-1R was abundantly expressed in human prostate cancer tissue and colocalized with P504S/α-methylacyl-CoA racemase, a marker of prostate cancer (27). This observation suggests that GLP-1R is predominantly expressed in cancerous cells in the prostate. We observed a similar pattern of GLP-1R expression in at least three sections of prostate tissue obtained from two independent nondiabetic patients with prostate cancer. Because the sensitivity and specificity of the available anti–GLP-1R antibodies are currently under discussion (28), the specificity of the anti–GLP-1R antibody used in this study was confirmed using GLP-1R–overexpressing COS-7 cells (Supplementary Fig. 1). Drucker (29) has demonstrated that the anti–GLP-1R antibody produced by Novus (1940002), but not that by Abcam (ab39072), can detect GLP-1R expression. We also tried to stain GLP-1R–overexpressing cells with the Abcam antibody ab39072. However, we did not observe any staining (Supplementary Fig. 1).

Ex-4 Inhibits Prostate Cancer Cell Proliferation Through GLP-1R

We next examined the in vitro effect of Ex-4 on the prostate cancer cell lines LNCap, PC3, ALVA-41, and DU145. LNCap and ALVA-41 are androgen dependent, whereas PC3 and DU145 are androgen independent. Treatment with Ex-4 (0.1–10 nmol/L) significantly decreased the proliferation of LNCap, PC3, and DU145 cells in a dose-dependent manner (Fig. 2*A*, *B*, and *D*), although it had the strongest effect on LNCap cells. In contrast, Ex-4 did not affect the proliferation of ALVA-41 cells (Fig. 2*C*). To determine whether the antiproliferative effect of Ex-4 on prostate cancer cells was mediated via GLP-1R, we examined its expression in these cells. Following a previous report (26), we first performed RT-PCR on the 890-BP coding sequence of *GLP-1R* to confirm the exact expression of the gene. *GLP-1R* mRNA was abundantly expressed in LNCap and DU145 cells, but was

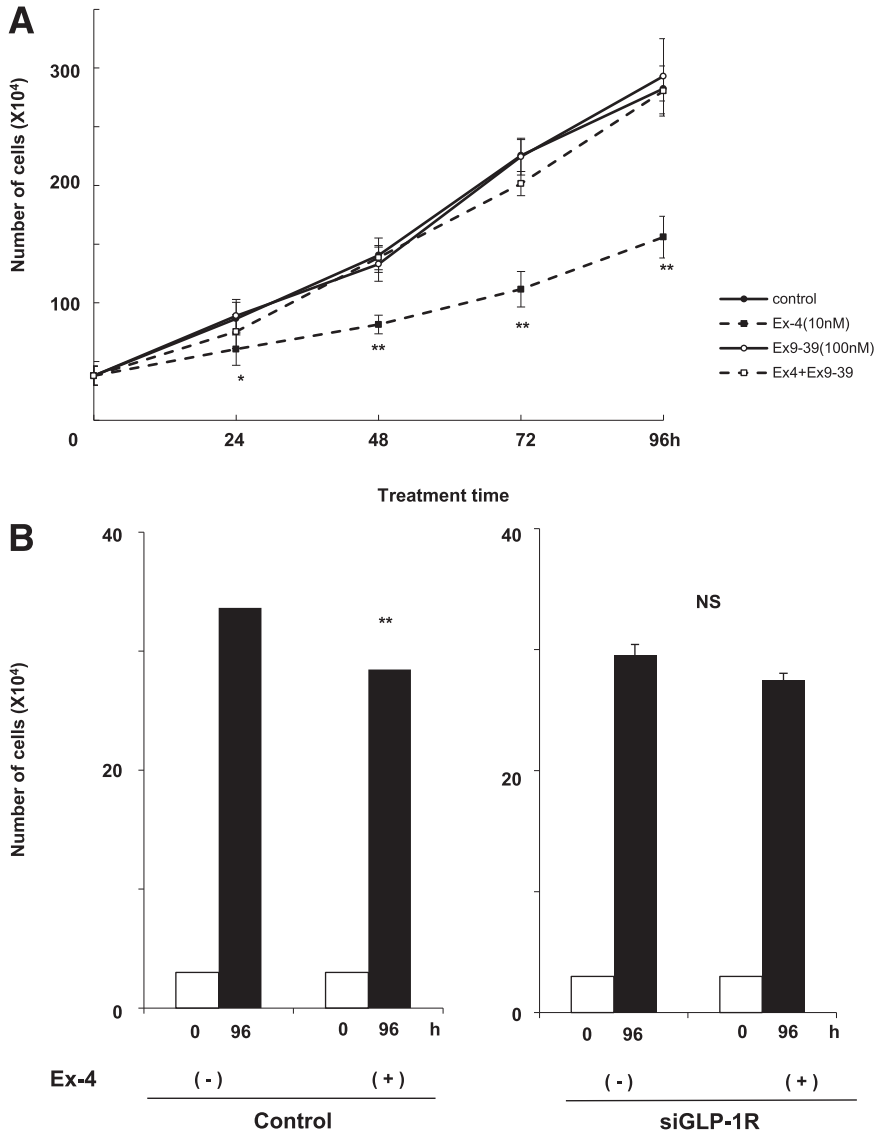

Figure 4— Ex-4 attenuates prostate cancer cell proliferation through GLP-1R. *A*: LNCap cells were maintained in media supplemented with 10% FBS with or without 10 nmol/L Ex-4 or 100 nmol/L Ex (9–39). After 0, 24, 48, 72, and 96 h, the cells were harvested, and cell proliferation was analyzed by cell counting using a hemocytometer. Control (nontreated), black circles with solid line; Ex-4 (10 nmol/L), black squares with dotted line; Ex (9–39) (100 nmol/L), white circles with solid line; Ex-4 (10 nmol/L) + Ex (9–39) (100 nmol/L), white squares with dotted line. One-way ANOVA was performed to calculate statistical significance: $^{*}P < 0.05$ vs. control, $^{**}P < 0.01$ vs. control. *B*: LNCap cells were transfected with either negative control duplexes or *GLP-1R* siRNA and maintained in media supplemented with 10% FBS with or without 10 nmol/L Ex-4. After 0 or 96 h, the cells were harvested, and cell proliferation was analyzed by cell counting using a hemocytometer. One-way ANOVA was performed to calculate statistical significance: $^{**}P < 0.01$ vs. control without Ex-4. *C*: Intracellular cAMP concentrations were measured at 0, 15, 30, and 60 min after 10 nmol/L Ex-4 stimulation. Unpaired *t* tests were performed to calculate statistical significance: $^{*}P < 0.05$ vs. 0 min, $^{**}P < 0.01$ vs. 0 min. *D*: LNCap cells were maintained in media supplemented with 10% FBS with or without 10 nmol/L Ex-4 or 10 μmol/L $PKI_{14–22}$. After 0, 24, 48, 72, and 96 h, the cells were harvested, and cell proliferation was analyzed by cell counting using a hemocytometer. Control (nontreated), black circles with solid line; Ex-4 (10 nmol/L), black squares with dotted line; $PKI_{14–22}$ (10 μmol/L), white circles with solid line; Ex-4 (10 nmol/L) + $PKI_{14–22}$ (10 μmol/L), white squares with dotted line. One-way ANOVA was performed to calculate statistical significance: $^{**}P < 0.01$ vs. control.

significantly lower in PC3 and ALVA-41 cells (Fig. 3*A*). Moreover, the sequence of the PCR product was compatible with that of the human *GLP-1R* cDNA as tested by direct sequencing. Quantitative real-time RT-PCR analysis further showed that *GLP-1R* expression was significantly higher in LNCap cells, followed by DU145 cells, compared with that in the other tested cells (Fig. 3*B*). Consistently, immunohistochemistry analysis revealed that GLP-1R protein expression was also higher in LNCap cells compared with that in the other tested cells. Indeed, counting the positively stained cells confirmed that GLP-1R protein expression was significantly greater in LNCap cells, followed by DU145 cells, compared with that in the other cell lines (Fig. 3*C* and *D*). Accordingly, we speculated that

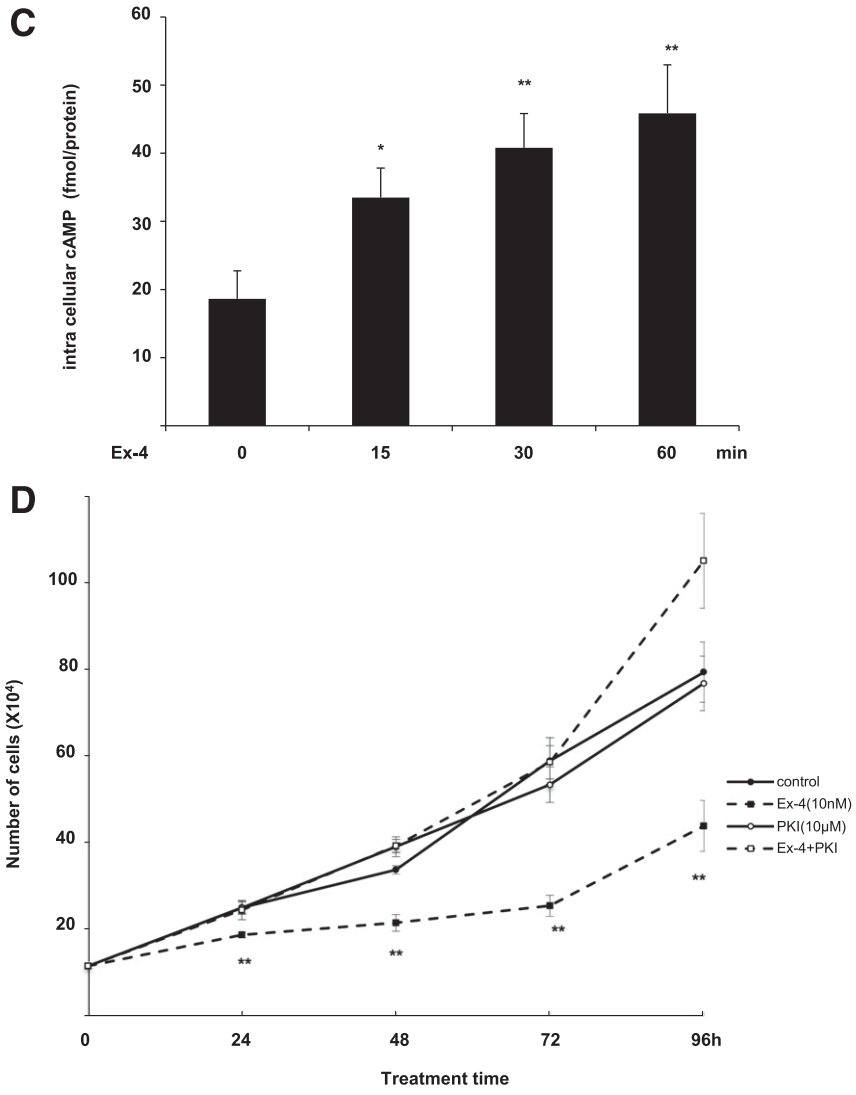

Figure 4—*Continued*.

the stronger suppression of cell proliferation by Ex-4 observed in LNCap cells compared with that in the other prostate cancer cells was caused by its higher GLP-1R expression. Consequently, the subsequent experiments were conducted with LNCap cells.

The antiproliferative effect of Ex-4 was completely abolished by the GLP-1R antagonist, Ex (9–39) in LNCap cells (Fig. 4*A*). Similarly, when *GLP-1R* was partially knocked down with siRNA, Ex-4–induced inhibition of cell proliferation was significantly impaired ($P < 0.01$; Fig. 4*B*). These data suggest that Ex-4 inhibited prostate cancer cell proliferation through GLP-1R activation. To elucidate whether the detected GLP-1R in LNCap cells can functionally activate downstream canonical signaling, we measured $[cAMP]_i$ after Ex-4 stimulation. Ex-4 significantly increased $[cAMP]_i$ in LNCap cells (Fig. 4*C*), but not in the other cell lines, while the basal cAMP concentration was higher in PC3 cells (Supplementary Fig. 3), suggesting that GLP-1R is functionally intact and responsive to Ex-4 in LNCap cells. Furthermore, the antiproliferative effect of Ex-4 was canceled by the PKA inhibitor $PKI_{14–22}$ (Fig. 4*D*) and forskolin-inhibited LNCap cell proliferation (Supplementary Fig. 4*A*), suggesting that Ex-4 inhibits cell proliferation through the canonical GLP-1R signal.

Ex-4 Does Not Decrease AR Activation

Prostate cancer cell proliferation depends mainly on AR activation. Thus, we investigated whether the antiproliferative effects of Ex-4 are caused by decreased AR action. PSA is one of the most important targets of AR activation in prostate cancer cells. As shown in Fig. 5*A* and *B*, DHT treatment profoundly stimulated PSA mRNA and protein expression in LNCap cells ($P < 0.01$) independent of Ex-4 concentration. However, while Ex-4 did not affect *PSA* mRNA expression, it significantly increased PSA protein production ($P < 0.01$). We next examined transcriptional activation of AR using a reporter assay. As described previously (22), pGL3-MMTV, which has multiple AR

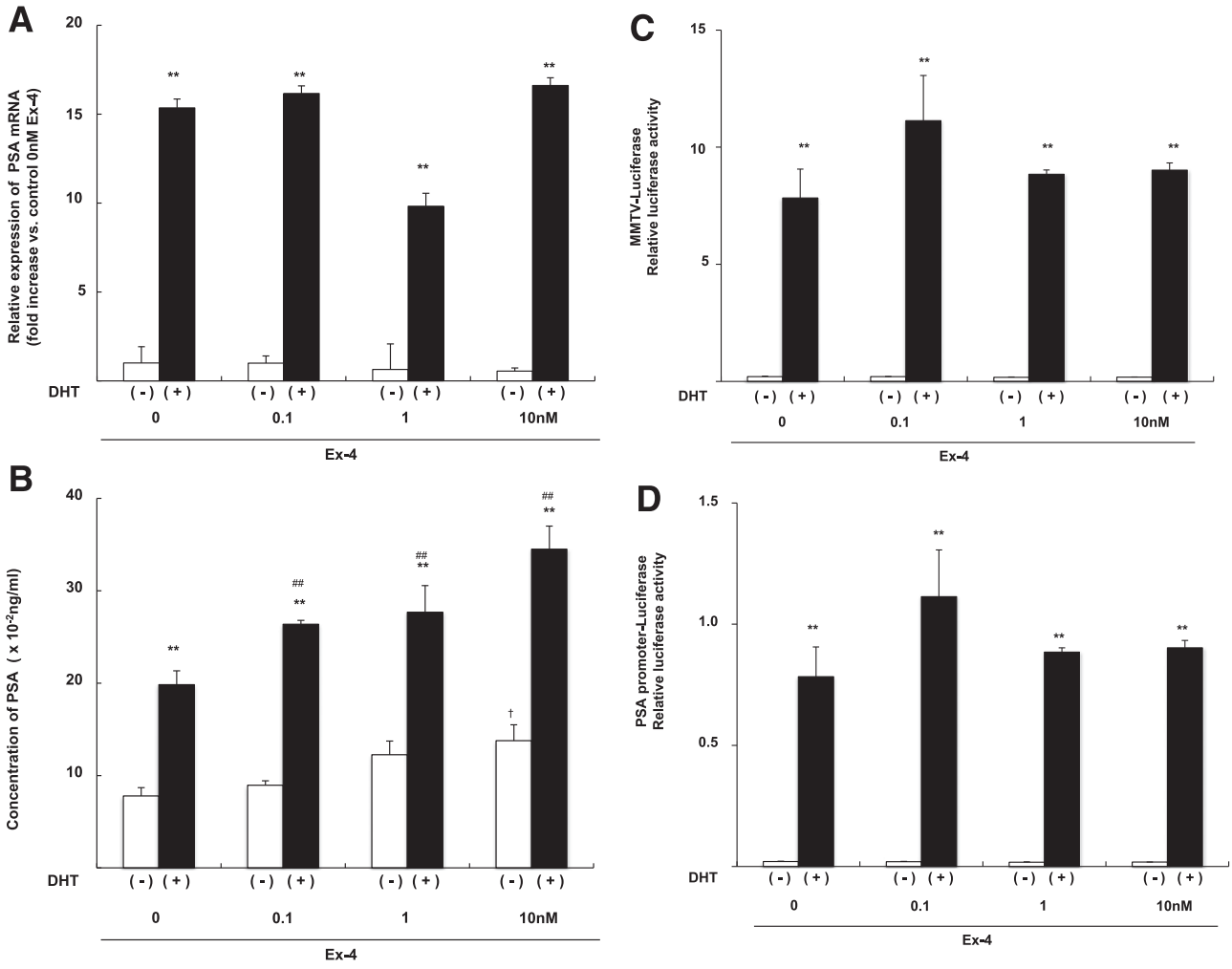

Figure 5—Ex-4 does not suppress AR activation. *A*: LNCap cells maintained in media supplemented with 10% charcoal-filtered FBS in 24-well plates were stimulated with 10^{-8} mol/L DHT or vehicle for 24 h. RNA was isolated, and quantitative RT-PCR was performed to examine *PSA* mRNA expression. *B*: PSA protein secreted into the culture medium was assayed by EIA. LNCap cells were transiently transfected with pGL3-MMTV (*C*) or pPSA-LUC (*D*) and maintained in media supplemented with 10% charcoal-filtered FBS with or without Ex-4 (0.1–10 nmol/L) for 12 h followed by stimulation with 10^{-8} mol/L DHT or solvent (ethanol) for 24 h. Luciferase activity was then measured. Unpaired *t* tests were performed to calculate statistical significance: $^{**}P < 0.01$ vs. DHT(−); $^{\#\#}P < 0.05$ vs. DHT(+), Ex-4(−); †$P < 0.05$ vs. DHT(−), Ex-4(−). Transfection efficiency was adjusted by normalizing firefly luciferase activities to *Renilla* luciferase activities.

activation sites in its promoter region (30,31), and the *PSA* promoter Luc were transfected into LNCap cells. As shown in Fig. 5*C* and *D*, whereas the AR transactivation activity was dramatically induced by DHT, Ex-4 treatment had no effect. These data strongly suggest that Ex-4 inhibits prostate cancer cell proliferation in a manner independent of AR transactivation. We also performed these experiments with a lower dose of DHT, 10^{-9} mol/L, and observed results similar to those shown in Fig. 5*A*–*D* (data not shown).

Ex-4 Suppresses Prostate Cancer Cell Proliferation Through Inhibition of ERK-MAPK

We next examined the mechanism by which Ex-4 inhibits prostate cancer cell proliferation. First, we performed BrdU incorporation assays to assess DNA synthesis. Ex-4 treatment for 24 h significantly decreased DNA synthesis in LNCap cells in a dose-dependent manner (Fig. 6*A*). However, Ex-4 did not induce apoptosis (Fig. 6*B*). The ERK-MAPK pathway is one of the main signaling pathways that stimulate cell proliferation in prostate cancer cells (32). Therefore, we examined whether Ex-4 attenuates ERK-MAPK activation. Ex-4 significantly reduced ERK-MAPK activation as determined by Western blot analysis of phospho-ERK1/2 in LNCap cells (Fig. 6*C*), but this effect was not observed in other prostate cancer cells (Supplementary Fig. 5). Next, we examined the effect of PKI on the inhibitory effect of Ex-4 on ERK-MAPK activation. As shown in Fig. 6*D*, the inhibitory effect of Ex-4 on ERK-MAPK activation was completely abolished by PKI. Moreover, forskolin inhibited ERK-MAPK phosphorylation in LNCap cells (Supplementary Fig. 5*B*). Interestingly, Ex-4 further inhibited LNCap cell proliferation when coincubated with 10 μmol/L PD98059 (Fig. 6*E*), a MAPK/ERK kinase (MEK) inhibitor, and a higher dose of PD98059

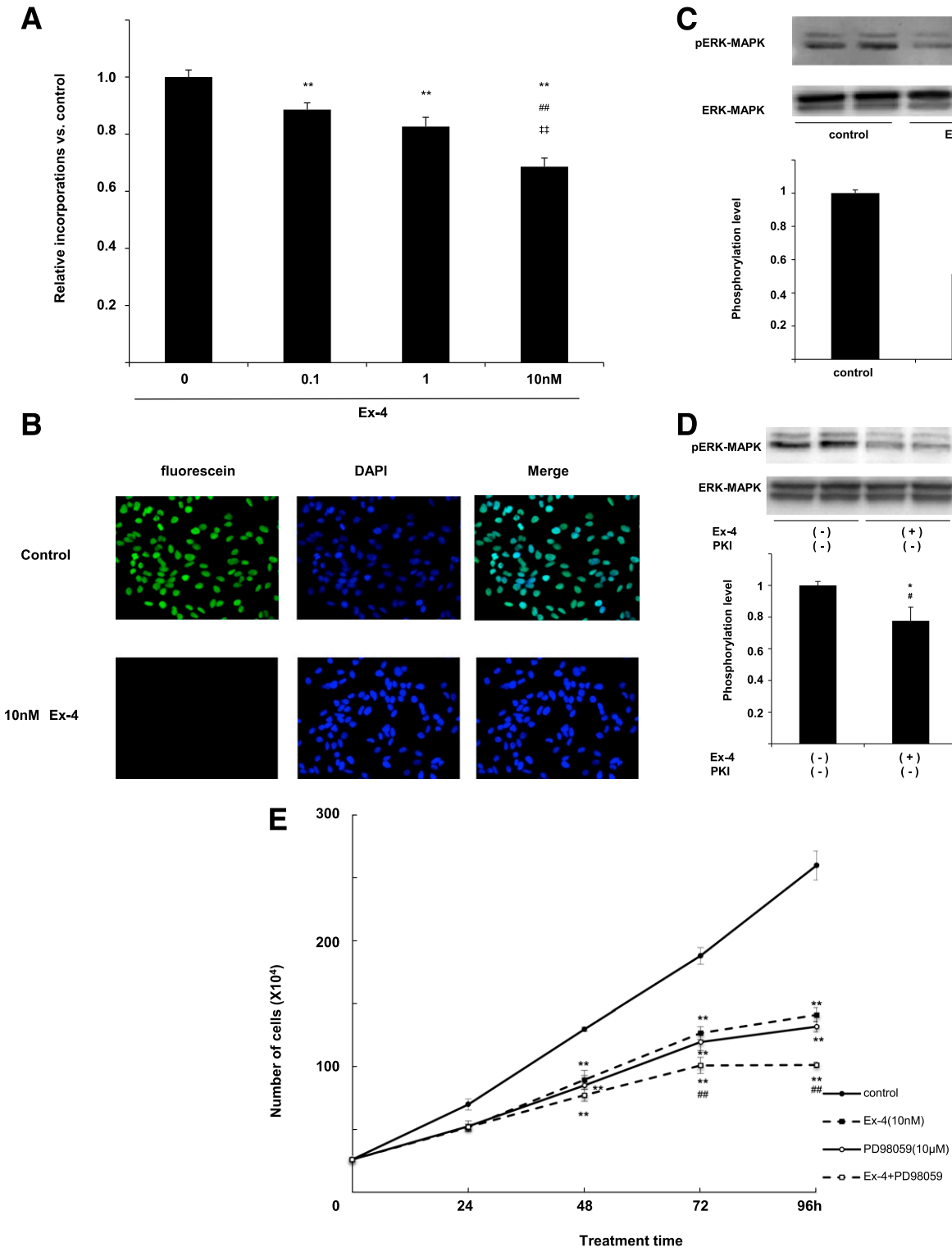

Figure 6—Ex-4 suppresses prostate cancer cell proliferation through inhibition of ERK-MAPK. *A*: LNCap cells were plated at a density of 3,000 cells/well in 96-well plates in media supplemented with 10% FBS and incubated with Ex-4 (0–10 nmol/L) for 24 h. BrdU solution was added during the last 4 h, and cells were harvested for measurement of DNA synthesis using a microplate reader at 450–620 nm. Mean data are expressed as a ratio of the control cell proliferation. Unpaired *t* tests were performed to calculate statistical significance: $^{**}P < 0.01$ vs. control; $\#\#P < 0.01$ vs. 0.1 nmol/L Ex-4; $‡‡P < 0.01$ vs. 1 nmol/L Ex-4. *B*: LNCap cells were plated on glass coverslips in 6-well plates. After incubation with 10 nmol/L Ex-4 or 1 unit/100 μL RQ1 DNase for 24 h, apoptotic cells were detected with TUNEL staining. The images shown are representative of triplicate independent experiments. *C*: LNCap cells maintained in media with 10% FBS were stimulated with 10 nmol/L Ex-4 or saline solution for 15 min. Cell lysates were harvested and subjected to Western blotting to assess phospho–ERK-MAPK and ERK-MAPK expression. Phospho–ERK-MAPK/ERK-MAPK protein levels were quantified by densitometry. Data were calculated from triplicate independent experiments and are shown as a ratio with the control. Unpaired *t* tests were performed to calculate statistical significance: $^{*}P < 0.05$ vs. control. *D*: LNCap cells maintained in media with 10% FBS were treated with 10 μmol/L $PKI_{14–22}$ or vehicle for 30

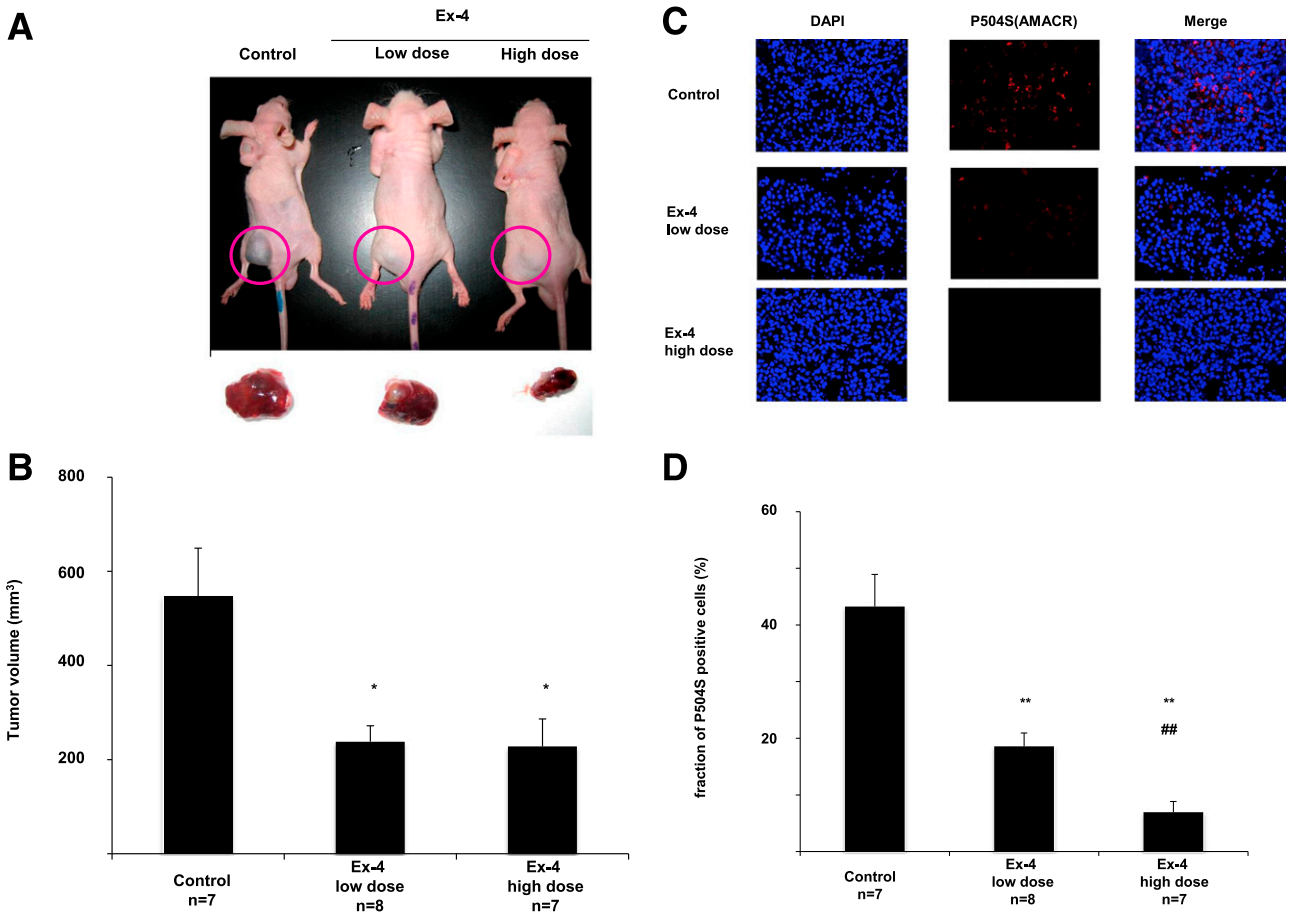

Figure 7—Ex-4 attenuates prostate cancer growth in vivo. *A*: Athymic CAnN.Cg-*Foxn1nu*/CrlCrlj mice (6 weeks of age) were transplanted with 1×10^6 LNCap cells (passages 4–8) and treated with vehicle ($n = 7$), high-dose Ex-4 (24 nmol/kg body weight/day; $n = 7$), or low-dose Ex-4 (300 pmol/kg body weight/day; $n = 8$). Tumors were imaged at 12 weeks of age. *B*: Tumor volume was calculated with the modified ellipsoid formula. One-way ANOVA was performed to calculate statistical significance: $^*P < 0.05$ vs. control. Sections (5 μm) were subjected to immunohistochemistry for P504S (*C*), Ki67 (*E*), phosphor–ERK-MAPK (*G*), or P504S and GLP-1R (*I*) and counterstained with DAPI. Original magnification ×400. P504S (*D*), Ki67 (*F*), phospho–ERK-MAPK (*H*), and GLP-1R–positive (*J*) cells were quantified by analyzing the fraction of stained cells in the tumor relative to the total number of nuclei. Values are expressed as a percentage of positive cells. Unpaired *t* tests were performed to calculate statistical significance: $^{**}P < 0.01$ vs. control; $\#\#P < 0.01$ vs. low-dose Ex-4.

completely abolished LNCap cell proliferation regardless of the Ex-4–induced antiproliferative effect (Supplementary Fig. 4*B*), suggesting that the Ex-4–induced inhibition of ERK-MAPK is independent of MEK inhibition.

These data indicate that Ex-4 suppresses prostate cancer cell proliferation mainly through the inhibition of ERK-MAPK via the cAMP-PKA pathway, but does not induce apoptosis.

Ex-4 Attenuates Prostate Cancer Growth In Vivo

Finally, to examine the anti–prostate cancer effect of Ex-4 in vivo, we transplanted LNCap cells into athymic mice. Six weeks after subcutaneous transplantation of LNCap cells into the flank region of mice, massive tumor formation was observed. However, tumor size was dramatically decreased in mice treated with Ex-4 (Fig. 7*A*). Calculation of tumor size using the modified ellipsoid formula

min before the addition of 10 nmol/L Ex-4 for 15 min. Cell lysates were harvested and subjected to Western blotting to assess phospho–ERK-MAPK and ERK-MAPK. Phospho–ERK-MAPK/ERK-MAPK protein levels were quantified by densitometry. Data were calculated from four independent experiments and are shown as a ratio of the PKI(−), Ex-4(−). Unpaired *t* tests were performed to calculate significance: $^*P < 0.05$ vs. PKI(−), Ex-4(−); $\#P < 0.05$ vs. PKI(+), Ex-4(+). *E*: LNCap cells were maintained in media supplemented with 10% FBS with or without Ex-4 (10 nmol/L) and 10 μmol/L PD98059. After 0, 24, 48, 72, and 96 h, the cells were harvested, and cell proliferation was analyzed by cell counting using a hemocytometer. Control (nontreated), black circles with solid line; Ex-4 (10 nmol/L), black squares with dotted line; PD98059 (10 μmol/L), white circles with solid line; Ex-4 (10 nmol/L) + PD98059 (10 μmol/L), white squares with dotted line. One-way ANOVA was performed to calculate statistical significance: $^{**}P < 0.01$ vs. control; $\#\#P < 0.01$ vs. Ex-4 or PD98059.

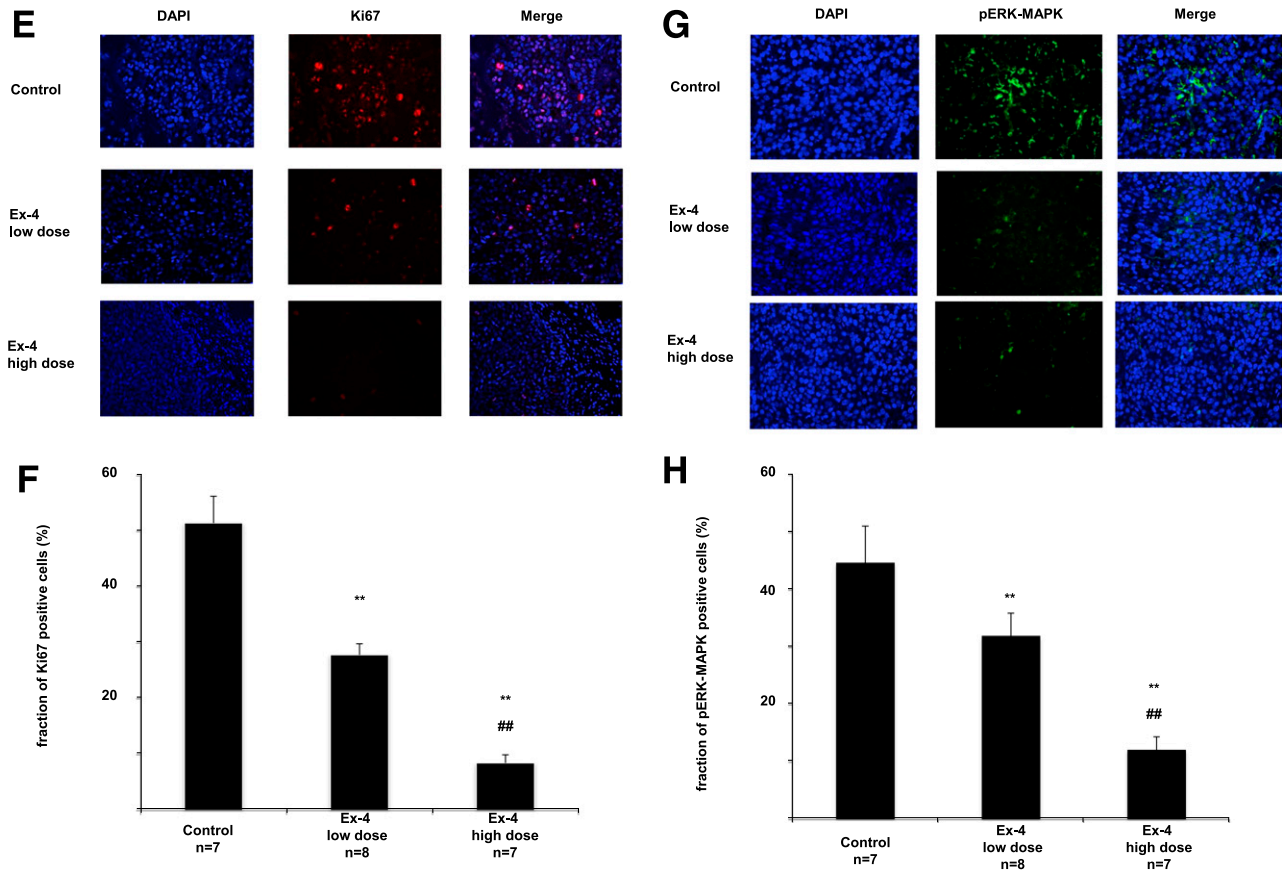

Figure 7—*Continued*.

revealed that Ex-4 decreased tumor size to almost half that of the control (Fig. 7*B*). As shown in Table 1, body weight and blood glucose levels were not changed by Ex-4 treatment. Compared with the control, plasma PSA levels were decreased in mice treated with Ex-4, although this effect was not statistically significant (control vs. low dose, $P = 0.11$; control vs. high dose, $P = 0.08$). Immunohistochemical analysis of paraffin-embedded sections of subcutaneous prostate cancer tumors demonstrated that the expression of P504S, a marker of prostate cancer, dramatically decreased by Ex-4 treatment (Fig. 7*C*). Quantification of P504S expression based on the mean number of P504S-positive cells divided by the total number of nuclei confirmed that there was a significant dose-dependent decrease in P504S expression in tumors of Ex-4–treated mice compared with control mice (Fig. 7*D*). We next examined the expression of Ki67, a marker of cell proliferation and cell cycle progression. Ki67 expression, which was clearly localized within the nucleus, was suppressed by Ex-4 treatment in a dose-dependent manner (Fig. 7*E* and *F*). Furthermore, consistent with our in vitro data, phospho–ERK-MAPK was decreased by Ex-4 treatment (Fig. 7*G*), which occurred in a dose-dependent manner (Fig. 7*H*). In addition, GLP-1R expression was not changed by Ex-4 treatment in vivo (Fig. 7*I*). These data suggest that Ex-4 attenuates prostate cancer growth in vivo by the same mechanism that was observed in vitro (i.e., through the inhibition of ERK-MAPK signaling).

DISCUSSION

In the current study, we clearly demonstrated that the GLP-1R is expressed in human prostate cancer and that the GLP-1R agonist Ex-4 attenuates prostate cancer growth through the inhibition of ERK-MAPK activation both in vivo and in vitro. Recently, incretin therapy, which includes GLP-1R agonists and dipeptidyl peptidase-4I, has become a popular antidiabetic treatment throughout the world (33), including Japan (34). There are many benefits of incretin therapy, such as pancreatic β-cell preservation, lower risk of weight gain, and fewer hypoglycemic attacks (35). In addition, incretin is a therapeutic option for the treatment of type 2 diabetes, even during end-stage renal disease (36). Furthermore, incretin therapy is expected to have tissue-protective effects beyond its glucose-lowering capacity (1). However, the current considerable interest in incretin therapy has raised the issue of its long-term safety, including the risk of carcinogenesis.

In a previous report (37), a 13-week continuous exposure to liraglutide, a GLP-1R agonist, was associated with a marked increase in plasma calcitonin levels and thyroid C-cell hyperplasia in wild-type mice, but not in GLP-1R–deficient mice. Furthermore, GLP-1R expression has been

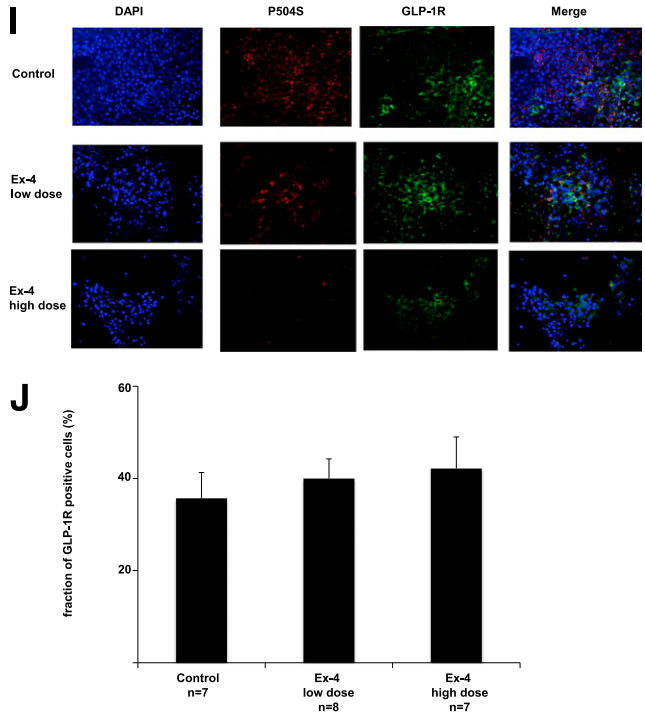

Figure 7—*Continued*.

detected in human neoplastic hyperplastic lesions of thyroid C cells (38). Thus, it can be speculated that these reports warn of a risk of carcinogenesis associated with incretin therapy. In contrast, two other studies (26,39) have demonstrated an anticancer effect of a GLP-1R agonist similar to that demonstrated in our study. Indeed, Koehler et al. (26) have clearly demonstrated an anti–colon cancer effect of Ex-4. Specifically, Ex-4 has been shown to increase intracellular cAMP levels and inhibit glycogen synthase kinase 3 and ERK-MAPK activation, leading to decreased colony formation and augmented apoptosis induced by irinotecan, a topoisomerase I inhibitor, in CT26 murine colon cancer cells (26). The cAMP-PKA pathway is a canonical signal transduction pathway downstream of GLP-1R, whose relationship with the ERK-MAPK pathway and cAMP is very complicated (40). Indeed, while induction of intracellular cAMP activates ERK-MAPK in some cell types, it inhibits it in others. In fact, GLP-1R signaling does not attenuate ERK-MAPK signaling in pancreatic cancer (41). In the current study using prostate cancer cells, the inhibitory effect of Ex-4 on ERK-MAPK activation was mediated by the cAMP-PKA pathway. This was demonstrated by the significantly increased cAMP levels in the highly GLP-1R–positive LNCap cells treated with Ex-4 (Fig. 4*C*), and by the PKI suppression of the Ex-4–mediated inhibition of ERK-MAPK (Fig. 6*D*).

In our previous study, we have observed that Ex-4 decreased vascular smooth muscle cell proliferation through AMPK activation (5), which is one of the mechanisms by which prostate cancer cell growth is inhibited (42). However, Ex-4 did not induce AMPK activation in prostate cancer cells (data not shown). Interestingly, an anti–breast cancer effect of Ex-4 has recently been reported (39). A similar mechanism by which Ex-4 attenuates cancer growth, namely the inhibition of ERK-MAPK, was confirmed by our data and a previous report (26), suggesting the importance of ERK-MAPK as a target of Ex-4 for decreasing cancer growth.

We also examined the effect of Ex-4 on another growth signal in prostate cancer, Akt phosphorylation; however, Ex-4 did not alter Akt activation in prostate cancer cells

Table 1—Characteristics of Ex-4–treated athymic mice after transplantation of LNCap cells

Characteristics	Control	Ex-4 (300 pmol/kg/day)	Ex-4 (24 nmol/kg/day)
Body weight (g)	22.6 ± 1.2	23.9 ± 0.9	21.9 ± 1.0
Plasma glucose (mg/dL)	128.6 ± 6.2	127.4 ± 11.4	135.8 ± 7.8
Plasma PSA (ng/mL)	6.2 ± 1.1	4.3 ± 0.8	3.9 ± 0.8

Data are presented as the mean ± SEM.

(Supplementary Fig. 6). Possibly, there is an MEK-ERK-MAPK–independent inhibitory mechanism by which Ex-4 inhibits prostate cancer cell proliferation, because PD98059 did not abolish the antiproliferative effect of Ex-4 (Fig. 6*E*), and a higher dose of PD98059 completely abolished prostate cancer cell proliferation (Supplementary Fig. 4*B*). However, our data suggest that Ex-4 inhibits prostate cancer cell proliferation mainly through ERK-MAPK inhibition. To fully elucidate the mechanism, further investigations are required.

We also observed that while Ex-4 inhibited prostate cancer cell proliferation, it did not affect apoptosis, as determined by the TUNEL assay (Fig. 6*B*). Indeed, further examination by Western blot analysis confirmed that Ex-4 did not affect apoptosis signals, such as caspase 3 activation, and induction of Bcl-2 and Bad, (Supplementary Fig. 6).

In addition, we observed that Ex-4 increased PSA protein expression in LNCap cells (Fig. 5*B*). The underlying molecular mechanism was not elucidated in this study; however, we have previously reported (22) that an interaction between GLP-1R signaling and FOXO1 may mimic AR activation, and another report (43) has demonstrated that Ex-4 induced the translocation of FOXO1 from the nucleus to the cytoplasm. Further study is thus required to explain how Ex-4 increased PSA protein levels.

In conclusion, we detected GLP-1R expression in samples of human prostate cancer tissue and cell lines, and demonstrated that Ex-4, a GLP-1R agonist, could attenuate prostate cancer growth through the inhibition of ERK-MAPK activation.

Duality of Interest. No potential conflicts of interest relevant to this article were reported.

Author Contributions. T.N. performed experiments, conceived the research hypothesis, wrote the manuscript, and approved the final manuscript. T.K., Y.H., and H.M. performed experiments and read and approved the final manuscript. S.I., M.Tanab., M.M., and K.N. provided the human prostate cancer tissues and read and approved the final manuscript. Y.Te., K.M., Y.Ts., R.N., T.T., and M.Tanak. assisted in patient recruitment, reviewed and edited the manuscript, and read and approved the final manuscript. T.Y. assisted in the conception of the research hypothesis, reviewed and edited the manuscript, and read and approved the final manuscript. T.Y. is the guarantor of this work and, as such, had full access to all the data in the study and takes responsibility for the integrity of the data and the accuracy of the data analysis.

References

1. Ussher JR, Drucker DJ. Cardiovascular biology of the incretin system. Endocr Rev 2012;33:187–215

2. Haffner SM, Lehto S, Rönnemaa T, Pyörälä K, Laakso M. Mortality from coronary heart disease in subjects with type 2 diabetes and in nondiabetic subjects with and without prior myocardial infarction. N Engl J Med 1998;339:229–234

3. Scheen AJ, Warzée F. Diabetes is still a risk factor for restenosis after drug-eluting stent in coronary arteries. Diabetes Care 2004;27:1840–1841

4. Arakawa M, Mita T, Azuma K, et al. Inhibition of monocyte adhesion to endothelial cells and attenuation of atherosclerotic lesion by a glucagon-like peptide-1 receptor agonist, exendin-4. Diabetes 2010;59:1030–1037

5. Goto H, Nomiyama T, Mita T, et al. Exendin-4, a glucagon-like peptide-1 receptor agonist, reduces intimal thickening after vascular injury. Biochem Biophys Res Commun 2011;405:79–84

6. Seshasai SR, Kaptoge S, Thompson A, et al.; Emerging Risk Factors Collaboration. Diabetes mellitus, fasting glucose, and risk of cause-specific death. N Engl J Med 2011;364:829–841

7. Hotta N, Nakamura J, Iwamoto Y, et al. Cause of death in Japanese diabetics based on the results of a survey of 18,385 diabetics during 1991-200—report of committee on cause of death in diabetes mellitus. J Japan Diab Soc 2007;50:47–61

8. Kasuga M, Ueki K, Tajima N, et al. Report of the JDS/JCA Joint Committee on Diabetes and Cancer. Diabetol Int 2013;4:81–96

9. Hirakawa Y, Ninomiya T, Mukai N, et al. Association between glucose tolerance level and cancer death in a general Japanese population: the Hisayama Study. Am J Epidemiol 2012;176:856–864

10. Morrison M. Pancreatic cancer and diabetes. Adv Exp Med Biol 2012;771:229–239

11. Joh HK, Willett WC, Cho E. Type 2 diabetes and the risk of renal cell cancer in women. Diabetes Care 2011;34:1552–1556

12. Yuhara H, Steinmaus C, Cohen SE, Corley DA, Tei Y, Buffler PA. Is diabetes mellitus an independent risk factor for colon cancer and rectal cancer? Am J Gastroenterol 2011;106:1911–1921

13. Xue F, Michels KB. Diabetes, metabolic syndrome, and breast cancer: a review of the current evidence. Am J Clin Nutr 2007;86:s823–s835

14. Esposito K, Chiodini P, Colao A, Lenzi A, Giugliano D. Metabolic syndrome and risk of cancer: a systematic review and meta-analysis. Diabetes Care 2012;35:2402–2411

15. Grossmann M, Wittert G. Androgens, diabetes and prostate cancer. Endocr Relat Cancer 2012;19:F47–F62

16. Kasper JS, Liu Y, Giovannucci E. Diabetes mellitus and risk of prostate cancer in the health professionals follow-up study. Int J Cancer 2009;124:1398–1403

17. Bonovas S, Filioussi K, Tsantes A. Diabetes mellitus and risk of prostate cancer: a meta-analysis. Diabetologia 2004;47:1071–1078

18. Mitin T, Chen MH, Zhang Y, et al. Diabetes mellitus, race and the odds of high grade prostate cancer in men treated with radiation therapy. J Urol 2011;186:2233–2237

19. Moses KA, Utuama OA, Goodman M, Issa MM. The association of diabetes and positive prostate biopsy in a US veteran population. Prostate Cancer Prostatic Dis 2012;15:70–74

20. Steering Committee of the Physicians' Health Study Research Group. Final report on the aspirin component of the ongoing Physicians' Health Study. N Engl J Med 1989;321:129–135

21. Ma J, Li H, Giovannucci E, et al. Prediagnostic body-mass index, plasma C-peptide concentration, and prostate cancer-specific mortality in men with prostate cancer: a long-term survival analysis. Lancet Oncol 2008;9:1039–1047

22. Fan W, Yanase T, Morinaga H, et al. Insulin-like growth factor 1/insulin signaling activates androgen signaling through direct interactions of Foxo1 with androgen receptor. J Biol Chem 2007;282:7329–7338

23. Eyre H, Kahn R, Robertson RM; American Cancer Society; the American Diabetes Association; the American Heart Association Collaborative Writing Committee. Preventing cancer, cardiovascular disease, and diabetes: a common agenda for the American Cancer Society, the American Diabetes Association, and the American Heart Association. Diabetes Care 2004;27:1812–1824

24. Gupta S, Wang Y, Ramos-Garcia R, Shevrin D, Nelson JB, Wang Z. Inhibition of 5α-reductase enhances testosterone-induced expression of U19/Eaf2 tumor suppressor during the regrowth of LNCaP xenograft tumor in nude mice. Prostate 2010;70:1575–1585

25. Nomiyama T, Nakamachi T, Gizard F, et al. The NR4A orphan nuclear receptor NOR1 is induced by platelet-derived growth factor and mediates vascular smooth muscle cell proliferation. J Biol Chem 2006;281:33467–33476

26. Koehler JA, Kain T, Drucker DJ. Glucagon-like peptide-1 receptor activation inhibits growth and augments apoptosis in murine CT26 colon cancer cells. Endocrinology 2011;152:3362–3372

27. Jiang Z, Woda BA, Rock KL, et al. P504S: a new molecular marker for the detection of prostate carcinoma. Am J Surg Pathol 2001;25:1397–1404
28. Pyke C, Knudsen LB. The glucagon-like peptide-1 receptor—or not? Endocrinology 2013;154:4–8
29. Drucker DJ. Incretin action in the pancreas: potential promise, possible perils, and pathological pitfalls. Diabetes 2013;62:3316–3323
30. Ham J, Thomson A, Needham M, Webb P, Parker M. Characterization of response elements for androgens, glucocorticoids and progestins in mouse mammary tumour virus. Nucleic Acids Res 1988;16:5263–5276
31. Adachi M, Takayanagi R, Tomura A, et al. Androgen-insensitivity syndrome as a possible coactivator disease. N Engl J Med 2000;343:856–862
32. Rodríguez-Berriguete G, Fraile B, Martinez-Onsurbe P, Olmedilla G, Paniagua R, Royuela M. MAP kinase and prostate cancer. J Signal Transduct 2012;2012:169170
33. Mikhail N. Safety of dipeptidyl peptidase 4 inhibitors for treatment of type 2 diabetes. Curr Drug Saf 2011;6:304–309
34. Nomiyama T, Akehi Y, Takenoshita H, et al.; CHAT. Contributing factors related to efficacy of the dipeptidyl peptidase-4 inhibitor sitagliptin in Japanese patients with type 2 diabetes. Diabetes Res Clin Pract 2012;95:e27–e28
35. Drucker DJ. Enhancing incretin action for the treatment of type 2 diabetes. Diabetes Care 2003;26:2929–2940
36. Terawaki Y, Nomiyama T, Akehi Y, et al. The efficacy of incretin therapy in patients with type 2 diabetes undergoing hemodialysis. Diabetol Metab Syndr 2013;5:10
37. Madsen LW, Knauf JA, Gotfredsen C, et al. GLP-1 receptor agonists and the thyroid: C-cell effects in mice are mediated via the GLP-1 receptor and not associated with RET activation. Endocrinology 2012;153:1538–1547
38. Gier B, Butler PC, Lai CK, Kirakossian D, DeNicola MM, Yeh MW. Glucagon like peptide-1 receptor expression in the human thyroid gland. J Clin Endocrinol Metab 2012;97:121–131
39. Ligumsky H, Wolf I, Israeli S, et al. The peptide-hormone glucagon-like peptide-1 activates cAMP and inhibits growth of breast cancer cells. Breast Cancer Res Treat 2012;132:449–461
40. Stork PJ, Schmitt JM. Crosstalk between cAMP and MAP kinase signaling in the regulation of cell proliferation. Trends Cell Biol 2002;12:258–266
41. Koehler JA, Drucker DJ. Activation of glucagon-like peptide-1 receptor signaling does not modify the growth or apoptosis of human pancreatic cancer cells. Diabetes 2006;55:1369–1379
42. Zadra G, Priolo C, Patnaik A, Loda M. New strategies in prostate cancer: targeting lipogenic pathways and the energy sensor AMPK. Clin Cancer Res 2010;16:3322–3328
43. Kodama S, Toyonaga T, Kondo T, et al. Enhanced expression of PDX-1 and Ngn3 by exendin-4 during beta cell regeneration in STZ-treated mice. Biochem Biophys Res Commun 2005;327:1170–1178